

QUT Digital Repository:
<http://eprints.qut.edu.au/>



Frost, Ray L. and Daniel, Lisa M. and Zhu, Huaiyong (2008) Laponite-supported titania photocatalysts. *Journal of Colloid and Interface Science* 322(1):pp. 190-195.

© Copyright 2008 Elsevier

Laponite-supported titania photocatalysts

Lisa M. Daniel, Ray L. Frost* and Huai Yong Zhu

Inorganic Materials Research Program, School of Physical and Chemical Sciences, Queensland University of Technology, GPO Box 2434, Brisbane Queensland 4001, Australia. Email: r.frost@qut.edu.au

Abstract

This study builds on previous results published on the synthesis and characterisation of laponite-supported titania photocatalysts. Titania nanocrystals are prepared prior to addition to the clay dispersion, by a sol-gel synthesis incorporating a microwave hydrothermal step. In addition to previously examinations with XRD, TEM and FT-IR, the samples are further characterised with SEM, ^{29}Si NMR and BET N_2 sorption to gain an insight into the effect of Ti concentration and surface area on the photoactivity of the samples.

Keywords: Titania; Photocatalyst; Laponite; Colloid, Surfactant, Hydrothermal treatment.

1. Introduction

The investigation of methods to enhance the photoactivity of titania materials has attracted much attention due to its' ability to be used for the removal of environmental pollutants [1-6]. One such method of enhancement is the support of fine titania particles on an inorganic surface. As fine titania nanoparticles experience

an inherent degree of aggregation, stabilisation on a support medium can reduce this, whilst still allowing for the exposure of more active sites which may participate in a photoreaction. TiO₂ particles have been immobilised on silica nanospheres [7] and thin films [8-11], on Fe-filled carbon nanocapsules [12], within the interlayer spaces of pillared clays [4, 13] and on the surface of exfoliated clay sheets, such as laponite .

Laponite is a synthetic hectorite, which forms exfoliated silicate layers when dispersed in water [14]. It has a relatively small particle size, with a basic unit consisting of a layered hydrous magnesium silicate platelet of diameter 25-30 nm with a thickness of approximately 1 nm [15]. When laponite powder is dispersed in water, a strongly negative charge appears on the faces of the silicate sheets and a weak positive charge appears on the rim. As a result of these charges, Laponite exhibits face-edge aggregation which leads to relatively open, macroporous structures of aggregates, described as house-of-cards structures. By utilising a surfactant to prevent the formation of this house of cards structure, TiO₂ may be immobilised on the clay face and the surfactant removed via calcination.

The aim of this paper is to build on previous reported characterisations of laponite-supported titania, examining the elemental composition of the samples and the surface area and porosity, through the use of scanning electron microscopy (SEM) [16] and BET N₂ sorption experiments. The effect of Ti concentration and surface area on the photoactivity of the samples is examined.

1.1. Synthesis of titania nanoparticles

TiO₂ colloids were prepared by the hydrolysis of titanium tetraisopropoxide (TPT) in deionised water according to an experimental procedure described by Wilson et al [17]. Titanium tetraisopropoxide (62.5 cm³) and isopropanol (10.0 cm³) were combined in a drop funnel and added over a 10 minute period, with vigorous stirring, to ultrapure deionised water (375 cm³) in a flat-based conical flask. Upon completion of the addition, 69 % nitric acid (2.65 cm³) was added to the flask, and the resultant solution refluxed at 80 °C with continuous stirring for 18 hours.

The resultant colloidal solutions were obtained and transferred to a Teflon-lined polycarbonate vessel for microwave hydrothermal treatment. A MicroSynth Labstation microwave (1200 ± 50 W, 2.45 GHz, Milestone MLS) was used at a setting of 80 % power, with a pressure ramp from ambient to 60 psi over a 10 minute period, with a corresponding temperature of 145 °C. Temperature in the reaction vessel was automated by the ATC-FO fiber optic probe, and pressure was maintained by the APC-55E pressure control. The TiO₂ colloid was treated at this temperature and pressure for a 15 minute period, to yield a white suspension. For comparison, hydrothermal treatment of the TiO₂ colloid was also performed in an oven at 180 °C for 24 hours to yield a thick white suspension.

1.2. Dispersion of laponite

Laponite clay (Laponite RD) was obtained from Fernz Specialty Chemicals, Australia and used as received. The clay powder has the chemical formula,

$\text{Na}_{0.67}\text{K}_{0.01}(\text{Si}_{7.95}\text{Al}_{0.05})-(\text{Mg}_{5.48}\text{Li}_{0.38}\text{Ti}_{0.01})\text{O}_{20}(\text{OH}_4)$, a BET specific surface area of $336.7 \text{ m}^2/\text{g}$ and a cation exchange capacity of 55 meq per 100 g of clay.

Laponite clay (2 g) was added over a period of 5 minutes to ultrapure deionised water (100 cm^3) with continuous stirring. The suspension was stirred for approximately 30 minutes until it became transparent.

A non-ionic poly(ethylene oxide) surfactant, Tergitol 15S-5, with a general chemical formula of $\text{C}_{12-14}\text{H}_{25-29}\text{O}(\text{CH}_2\text{CH}_2\text{O})_5\text{H}$ and an average molecular weight of 420 g/mol was then added resulting in an opaque solution and stirring was continued for a further 30 minutes. The molar ratio of PEO to Laponite (moles PEO to moles Laponite) employed was 2:1.

1.3. *Preparation of TiO_2 -clay photocatalysts*

To the clay dispersions TiO_2 sol was added with Ti:clay ratios of 10, 20, 30 and 40mmol of Ti/g of clay. All samples were stirred for 3 hours, hydrothermally treated at 180°C for a period of 24 hours, upon which they were centrifuged, washed with deionised water and dried in an oven at 80°C . They were then calcined at 500°C for a period of 24 hours.

For comparison, samples prepared with 40mmol Ti/g were hydrothermally treated at temperatures of 180, 140 and 80°C and also without any hydrothermal treatment. The two most important parameters: hydrothermal temperature and Ti/Clay ratio were highlighted in the sample names. The number after the letters “Ti-L” indicates the Ti/Clay ratio in mmol of Ti per gram of clay (mmol/g), which are 10,

20, 30 and 40 respectively. The number at the end indicates the hydrothermal temperature. For instance, Ti-L10-180 is the sample prepared with a Ti/Clay ratio of 10 mmol/g and a hydrothermal temperature of 180 °C.

To examine the effect of the washing medium, samples prepared with 10 and 30 mmol Ti/g were washed with pure deionised water, or deionised water followed by ethanol. These samples were then dried at 80 °C and calcined at 500 °C for 24 hours.

1.4. *Scanning Electron Microscopy (SEM)*

X-ray microanalyses (EDX) of the samples were performed on a JEOL 840A analytical SEM (JEOL Ltd, Tokyo, Japan). Prior to analysis, pressed powder samples were coated with a thin layer of evaporated carbon for conduction and examined at 25 kV accelerating voltage using a standardless procedure on the JEOL 840 SEM equipped with a JEOL-2300 energy-dispersive X-ray microanalysis system (JEOL Ltd, Tokyo, Japan). Three measurements were recorded for each sample over a sample area of 2 mm².

1.5. *²⁹Si Nuclear Magnetic Resonance Spectroscopy*

²⁹Si NMR spectra were recorded on a double-channel Varian InfinityPlus 400 spectrometer, equipped with a 7.5 mm cross-polarization (CP)-MAS probehead, working at 79.44 MHz. ²⁹Si-single pulse excitation spectra were recorded for samples Laponite, Ti-LpH, Ti-LpH6 and Ti-LpH9 with a recycle delay of 100 s.

1.6. *BET N₂ Sorption*

The surface areas of the TiO₂-clay composites were calculated by the BET method using N₂ adsorption-desorption on a Micromeritics ASAP 2010 at a partial pressure range of 0.01 to 0.99. The mean pore size was determined via the t-plot method and the pore size distribution and pore volume were calculated using the Tristar software. The samples were degassed at 110 °C overnight prior to the analysis.

2. **Results**

2.1. *Scanning Electron Microscopy*

Table 1 shows the elemental compositional data for the hydrothermally treated samples prepared with varying Ti concentrations. It was found that the actual ratio of Ti concentration for the samples was approximately 20-25 % of the concentrations employed in the synthesis. Therefore for the sample prepared with 40 mmol Ti/g, the actual concentration obtained was only 11 mmol Ti/g.

2.2. *²⁹Si Nuclear Magnetic Resonance Spectroscopy*

In ²⁹Si-NMR spectroscopy, peaks are assigned the letters, Q_n, T_n, D_n, M_n, based on the number of oxygen atoms bonded to the Si atom, 4, 3, 2 and 1 respectively, where n is the number of oxygen atoms bonded to a further Si atom. In Figure 1 laponite exhibits two main peaks at -96 ppm and -86 ppm attributed to Q₃ and Q₂ sites respectively [18]. The Q₃ peaks arise from the Si(OMg)(OSi)₃ silicon

nuclei within the tetrahedral sheets. The Q_2 peak is attributed to the presence of silanols, $Si(OMg)(OSi)_2(OH)$, both at the broken edges of the clay sheet and due to defects within the clay structure.

In the sample Ti-L40-180, an increase in the intensity of the Q_2 peak compared to the Q_3 peak is observed in Figure 2. This is likely due to the removal of Q_3 $Si(OMg)(OSi)_3$ sites located on the clay faces, through the formation of Ti-O-Si bonds. The resolution of the Q_2 peak is also greater for Ti-L40-180 than for laponite, due to the lower water content brought about by calcination. In addition to the Q_2 peak at -86.2 ppm, further peaks are observed at -81.6, -83.6, -88.1 and -89.1 ppm. These peaks are believed to arise from the Q_2 $Si(OMg)(OSi)_2(OTi)$ species formed in the reaction, both on the face and on the edge of the clay plates.

2.3. *BET N₂ Sorption*

Laponite exhibits a type IV isotherm corresponding to a mesoporous solid, according to the BDDT classification of adsorption isotherms [19]. The IUPAC classification designates mesopores as those with widths between 2 and 50 nm. The adsorption isotherm of mesoporous solids contains a hysteresis loop caused by the capillary condensation that occurs within mesopores. The lower branch describes the progressive addition of gas to the system and the upper branch, the progressive withdrawal. The type of hysteresis loop can also determine the shape of the pores. The pores in laponite clay are designated slit-like in shape [19]. Laponite was found to possess a surface area of 361 m²/g, with almost one third of its surface area attributed to micropores. The IUPAC classification designates micropores as those

with widths smaller than 2 nm. The average pore size in the laponite sample was found to be approximately 3.1 nm, with the most common pore size at 3.9 nm.

Table 2 displays the N₂ sorption data for the samples prepared with varying Ti-clay ratios. Like laponite, the Ti-L samples exhibit type IV isotherms and have a similar overall surface area. However, the area attributed to micropores disappears from these samples, with the external surface area, showing a marked increase. The average pore sizes are also much higher between 5.7 and 6.8 nm in diameter. The pore size distribution of laponite and a representative sample, Ti-L40-180 can be seen in Figures 3 and 4 respectively. The pore size distribution is much larger for the Ti-L sample, with pores ranging from approximately 2-11 nm in diameter, indicating a more irregular, less ordered structure.

Table 3 displays the BET N₂ sorption data for the samples prepared with varying hydrothermal treatment temperatures. Increasing the hydrothermal treatment temperature appears to increase the average pore size, with averages ranging from 3.7 to 5.7 nm for the samples without hydrothermal treatment and that treated at 180 °C. The micropore component of the surface area is again absent in these samples, with only a minimal effect observed in the overall surface area.

Table 4 displays the N₂ sorption data for the samples washed with either water or ethanol prior to calcination. Once again, the micropore component of the surface area observed in pure laponite, is absent from these samples, whilst an increase in external surface area is observed. Ti-L30-noHT has the largest overall surface area of the samples examined. The average pore size is smaller for the sample washed with

ethanol. Upon examination of the pore size distribution plots of Ti-L30-noHT and Ti-L30-noHT-E in Figures 5 and 6, it can be seen that there is a significant difference in the relative amount of pores with diameters above and including 9 nm. The sample washed with water, exhibits a large degree of pores with a diameter of approximately 9 nm whereas, the sample washed with ethanol, does not.

3. Discussion

3.1. Location of Titania on Laponite surface

Previously published transmission electron microscopy images show the heterogeneous dispersion of titania nanoparticles on the faces of laponite plates. This is confirmed by ^{29}Si NMR spectra, which exhibits a reduction in the Q_3 peaks attributed to $\text{Si}(\text{OMg})(\text{OSi})_3$ sites located on the clay faces, through the formation of an Si-O-Ti bond with the titania nanoparticles and the clay face.

3.2. Effect of Titania Concentration

Previously reported photocatalytic tests showed that the samples prepared with varying Ti concentrations, caused the degradation of the dye, Sulphorhodamine B. The samples are ranked by the degree of degradation achieved over 90 minutes of irradiation by UV light, and are as follows: $\text{Ti-L40-180} > \text{Ti-L30-180} > \text{Ti-L10-180} > \text{Ti-L20-180}$ [16]. The Ti concentration was therefore found to have some effect on the photocatalytic activity of the sample, however there is no direct relationship present. This is highlighted in the graph in Figure 7. It is very likely that there is another factor at play affecting the photoactivity of the sample.

3.3. *Effect of Hydrothermal Treatment Temperature*

Increasing the hydrothermal treatment temperature of the Ti-clay dispersions has been reported in prior work to result in a slight increase in crystal size due to a process known as Ostwald ripening. Previously reported results of photoactivity tests, showed that the samples prepared with different hydrothermal treatment temperatures exhibited the following trend in photoactivity: Ti-L40-180 > Ti-L40-140 > Ti-L40-80 [16]. Titania is commonly reported to exhibit greatest activity with samples of smaller crystallite size, however, in this case, the larger samples produced by more severe hydrothermal treatment are the most photoactive. It is believed that the TiO₂ nanoparticles prepared via the microwave method are not fully crystalline and this additional hydrothermal treatment aids in improving their crystallinity and consequently their photocatalytic efficiency.

3.4. *Effect of Washing Medium*

The photocatalytic activity was reported to be higher in the samples that have been washed with water and not with ethanol. Ding et al. have reported that washing modified clays with ethanol prior to calcination can increase porosity, due to the reduction of interfacial tension that occurs by replacing water with ethanol within the pores [1]. In this case, however, a reduction in pore size was observed. This is believed to be due to the removal by ethanol of the PEO surfactant micelles which acts as templates [3]. Templating is the process in which surfactant micelles introduced into the clay structure and removed by calcination, leave behind pores that mimic the size and shape of the micelle [21].

Ti-L30-noHT has a significant number of pores with a diameter of 9 nm, the diameter of the PEO micelle, which are mostly absent from Ti-L30-noHT-E. Decreasing the pore size and surface area diminishes the photoactivity of the sample by reducing the accessibility of the dye molecules to the TiO₂ surface upon which the photocatalytic reaction takes place.

4. Conclusions

Laponite-supported TiO₂ photocatalysts were produced and a variety of synthesis parameters examined in this study. The photocatalytic activity of the samples was improved by increasing the Ti concentration to provide a greater number of active anatase sites; by the use of hydrothermal treatment of the Ti-laponite dispersion to enhance the anatase crystallinity; and lastly by increasing the surface area and pore size via surfactant templating, increasing the accessibility of the dye molecules to the anatase surface.

Acknowledgments

The financial and infra-structure support of the Queensland University of Technology, Inorganic Materials Research Program is gratefully acknowledged. The Australian Research Council (ARC) is thanked for funding the instrumentation.

References

1. Ding, Z., H.Y. Zhu, G.Q. Lu and P.F. Greenfield, *J. Colloid Interface Sci.* 209 (1999) 193-199.
2. J. Li, C. Chen, J. Zhao, H. Zhu and Z. Ding, *Appl. Catal. B: Environ.* 37 (2002) 331-338.
3. Zhu, H.Y., J.Y. Li, J.C. Zhao and G.J. Churchman, *Appl. Clay Sci.* 28 (2005) 79-88.
4. Ding, Z., H.Y. Zhu, G.Q. Lu, and P.F. Greenfield, *Encycl. Surface Colloid Sci.* (2002) 4030-4042.
5. Zhu, H., X. Gao, Y. Lan, D. Song, Y. Xi and J. Zhao, *J. Am. Chem. Soc.* 126 (2004) 8380-8381.
6. Zhu, H.Y., Y. Lan, X.P. Gao, S.P. Ringer, Z.F. Zheng, D.Y. Song and J.C. Zhao, *J. Am. Chem. Soc.* 127 (2005) 6730-6736.
7. Khalil, K.M.S., A.A. Elsamahy, and M.S. Elanany, *J. of Colloid Interface Sci.* 249 (2) (2002) 359-365.
8. Guan, K., *Surf. Coat. Technol.* 191 (2005) 155-160.
9. C.H. Kwon, J.H. Kim, I.S. Jung, H. Shin and K.H. Yoon, *Ceram. Int.* 29 (2003) 851-856.
10. W. Que, Z. Sun, Y. Zhou, Y.L. Lam, Y.C. Chan, and C.H. Kam, *Thin Solid Films*, 359 (2000) 177-183.
11. Z. Jiwei, Y. Tao, Z. Liangying, and Y. Xi, *Ceram. Int.* 25 (1999) 667-670.
12. W.-C. Huang, *Method of producing quantum-dot powder and film via templating by a two-dimensional ordered array of air bubbles in a polymer*, 2003.
13. J.L. Valverde, P. Sanchez, F. Dorado, C.B. Molina and A. Romero, *Micropor. Mesopor. Mater.* 54 (1-2) (2003) 155-165.
14. W. Li, M. Sirilumpen, and R.T. Yang, *Appl. Catal. B: Environ.* 11 (3-4) (1997) 347-363.
15. Hanley, H.J.M., C.D. Muzny, and B.D. Butler, *Langmuir*, 13 (20) (1997) 5276-5282.
16. L.M. Daniel, R.L. Frost and H.Y. Zhu, *J. Colloid Interface Sci.* 316 (2007) 72-79.
17. G.J. Wilson, A.S. Matijasevich, D.R.G Mitchell, J.C. Schulz, and G.D. Will, *Langmuir*, 22(5) (2006) 2016-2027.
18. Delevoye, L., J.L. Robert, J. Grandjean, *Clay Miner.* 38 (1) (2003) 63-69.

19. S.J. Gregg, K.S.W. Sing, Adsorption, Surface Area and Porosity, second ed., Academic Press, London, 1982.
20. J. Rouquerol, D. Avnir, C.W. Fairbridge, D.H. Everett, J.H. Haynes, N. Pernicone, J.D.F. Ramsay, K.S.W. Sing and K.K. Unger, Pure Appl. Chem. 66 (8) (1994) 1739-1758.
21. H.Y. Zhu, Z. Ding, J.C. Barry, J. Phys. Chem. B 106 (2002) 11420-11429.

List of Tables

Table 1 SEM-EDX compositional data for samples Ti-L10-180, Ti-L20-180, Ti-L30-180 and Ti-L40-180.

Table 2 BET N₂ sorption data for samples prepared with varying Ti concentrations.

Table 3 BET N₂ sorption data for samples prepared with varying hydrothermal treatment temperatures.

Table 4 BET N₂ sorption data for samples prepared with different washing media.

List of Figures

Figure 1 ^{29}Si NMR spectra of the Q₂ peaks of laponite.

Figure 2 ^{29}Si NMR spectra of the Q₂ peaks of Ti-L40-180.

Figure 3 Pore size distribution of laponite.

Figure 4 Pore size distribution of Ti-L40-180.

Figure 5 Pore size distribution of Ti-L30-noHT.

Figure 6 Pore size distribution of Ti-L30-noHT-E.

Figure 7 Graph of Ti concentration vs photoactivity

	Ti-L10-180	Ti-L20-180	Ti-L30-180	Ti-L40-180
O Atomic %	67.49	68.70	71.64	66.27
Mg Atomic %	11.86	11.10	9.69	8.75
Si Atomic %	16.62	14.42	12.11	12.01
Ti Atomic %	4.04	5.79	6.58	12.99
Mmol Ti/g clay	2.51	4.15	5.61	11.17
Yield (%)	25.10	20.73	18.70	27.93

Table 1

Sample Name	Isotherm Type	Surface Area (m ² /g)			Pore Diameter (nm)	
		BET	External	Micropore	Average	Most Common
Laponite	IV	361	258	102	3.1	3.9
Ti-L10-180	IV	352	334	17	6.8	7.4
Ti-L20-180	IV	335	328	7	5.9	6
Ti-L30-180	IV	354	354	0	6.1	5.9
Ti-L40-180	IV	330	330	0	5.7	5.0

Table 2

Sample Name	Isotherm Type	Surface Area (m ² /g)			Pore Diameter (nm)	
		BET	External	Micropore	Average	Most Common
Laponite	IV	361	258	102	3.1	3.9
Ti-L40noHT	IV	364	364	0	3.7	4.9
Ti-L40-80	IV	366	366	0	4.9	3.5 & 4.0
Ti-L40-140	IV	298	298	0	5.2	4.5
Ti-L40-180	IV	330	330	0	5.7	5.0

Table 3

Sample Name	Isotherm Type	Surface Area (m ² /g)			Pore Diameter (nm)	
		BET	External	Micropore	Average	Most Common
Laponite	IV	361	258	102	3.1	3.9
Ti-L30-180	IV	354	354	0	6.1	5.9
Ti-L30-noHT	IV	384	384	0	5.3	4.3
Ti-L30noHT-E	IV	335	335	0	4.7	3.6

Table 4

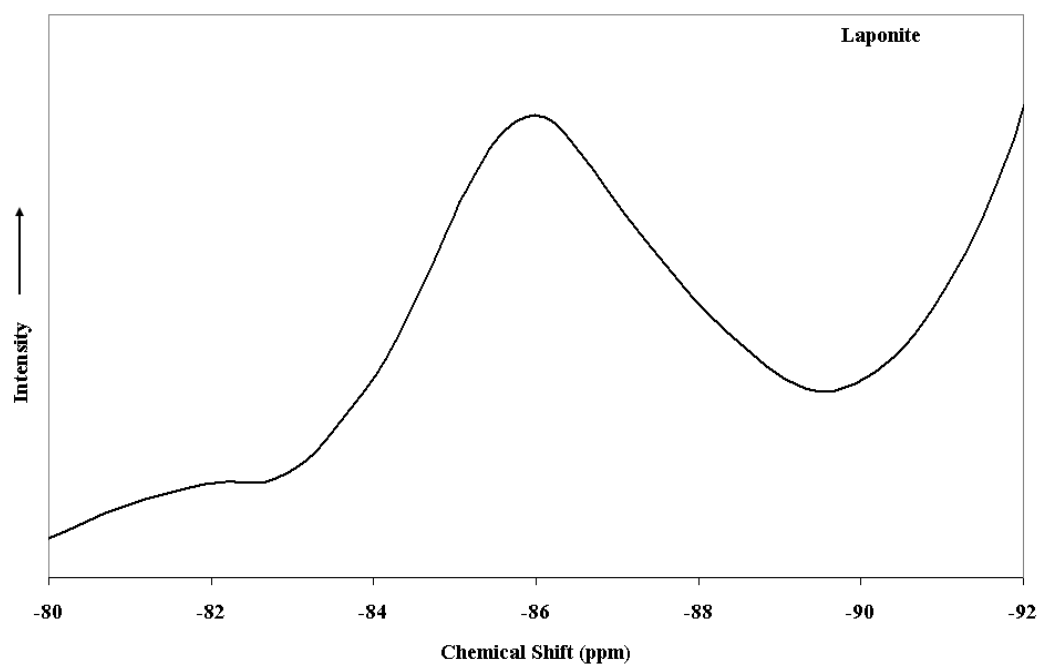


Figure 1

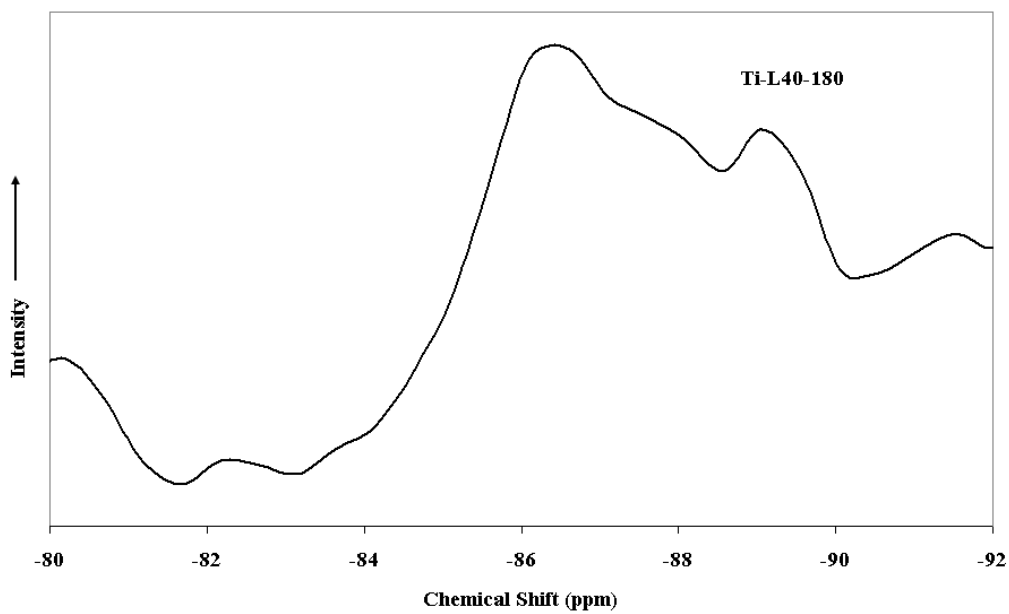


Figure 2

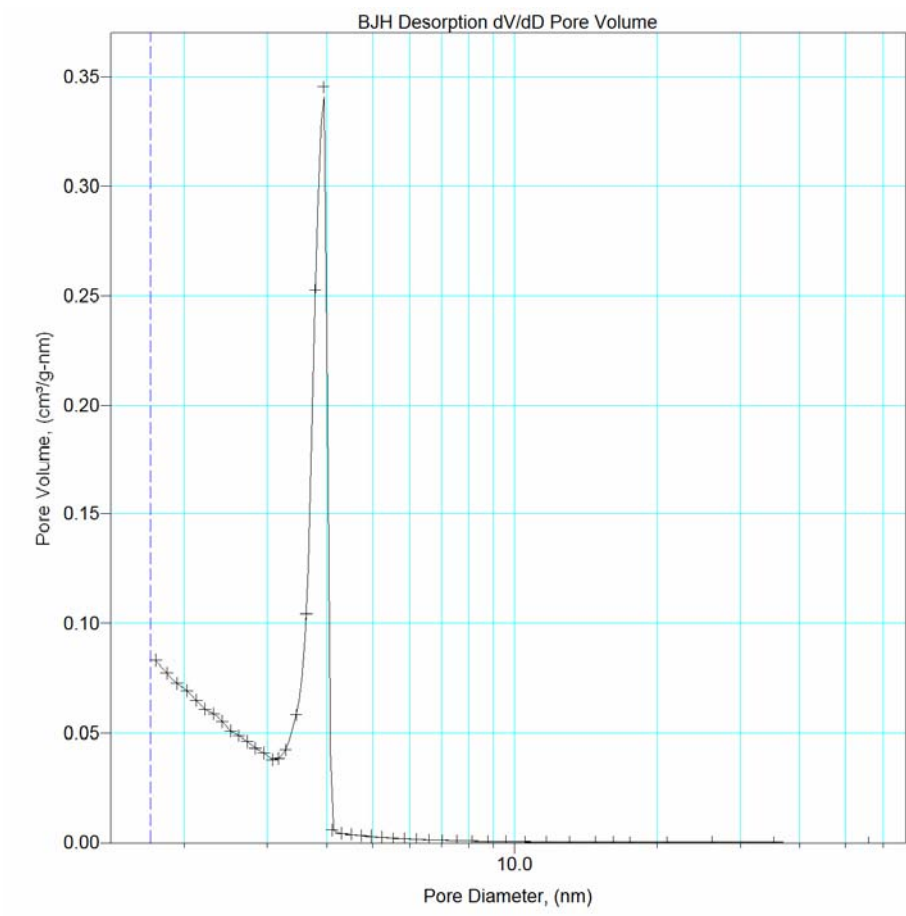


Figure 3

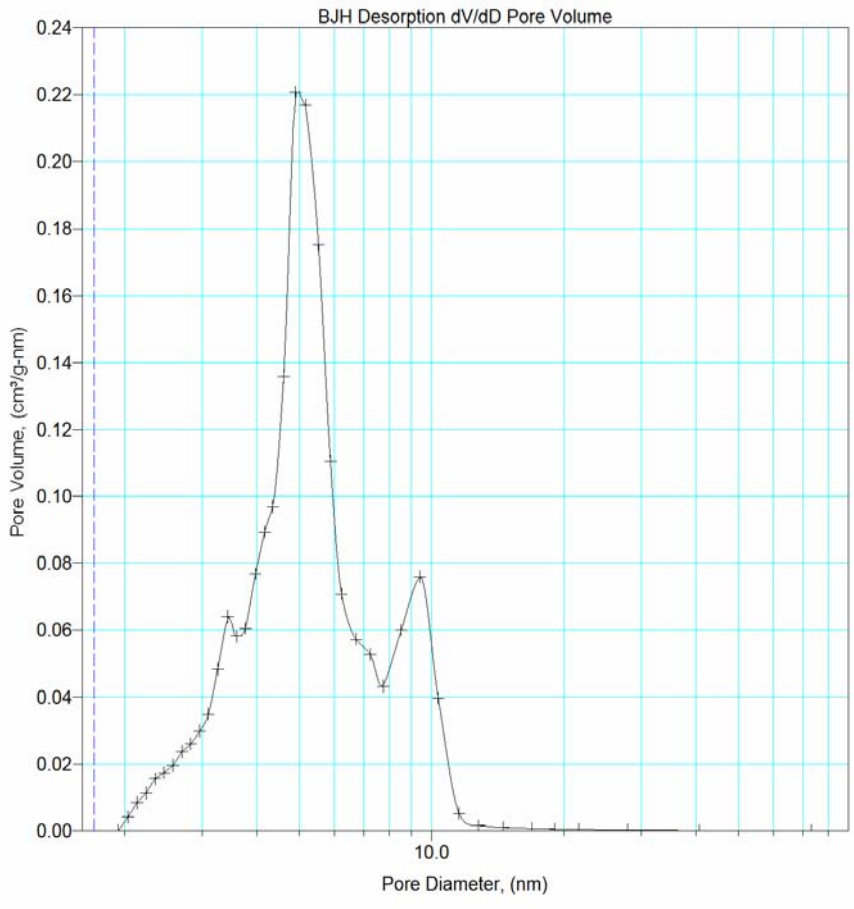


Figure 4

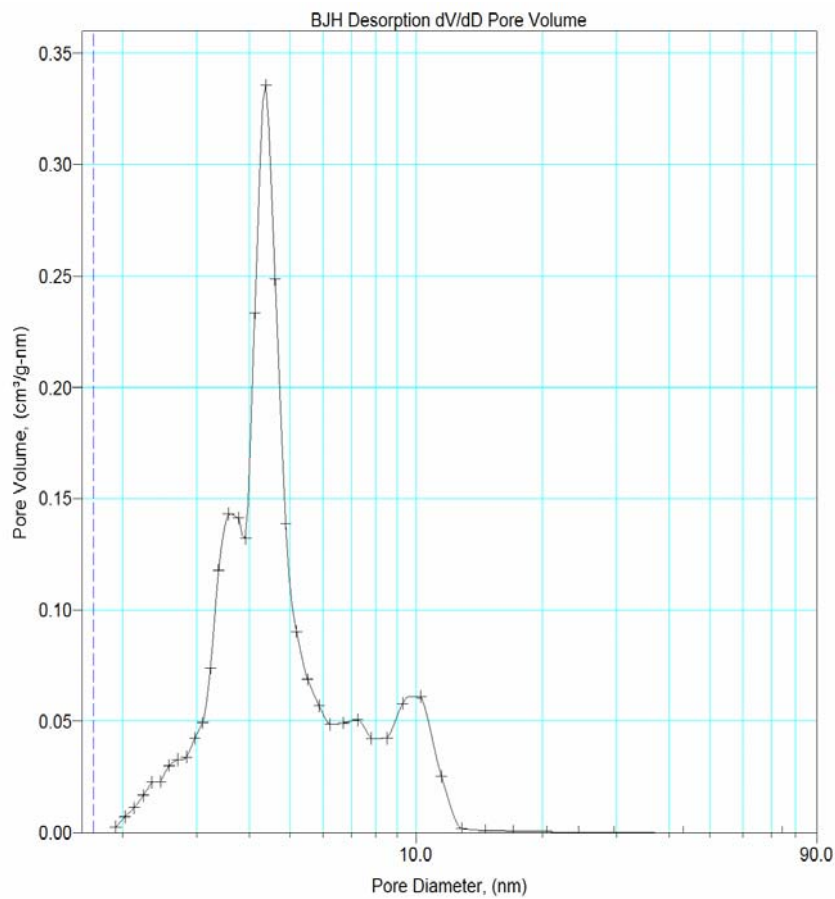


Figure 5

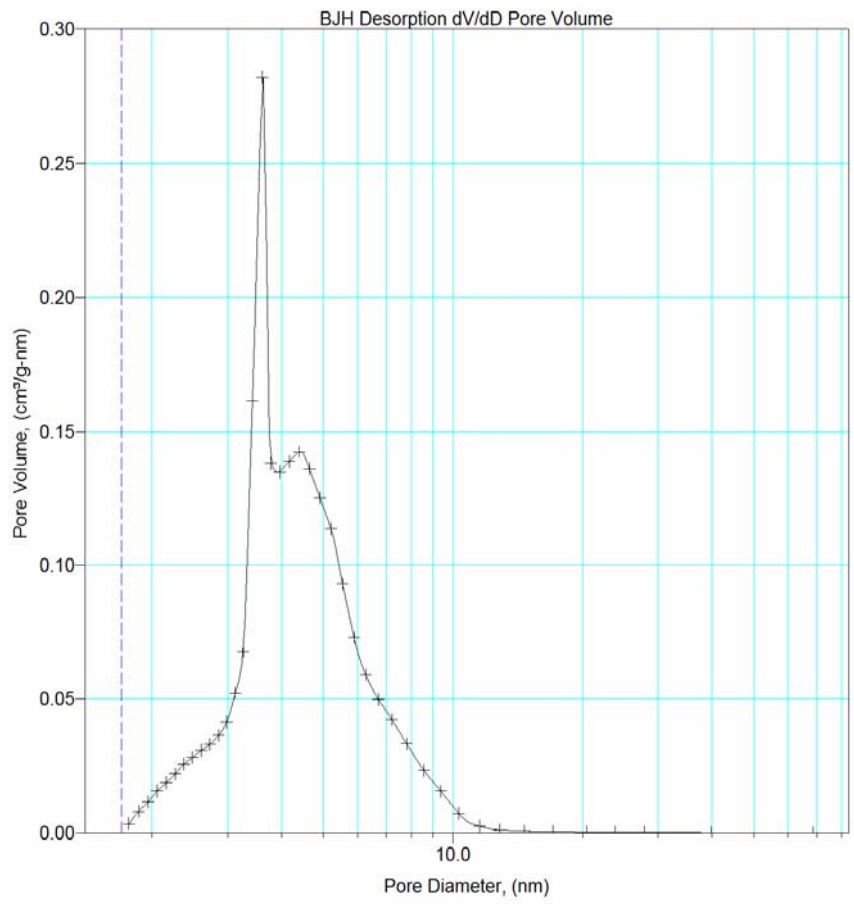


Figure 6

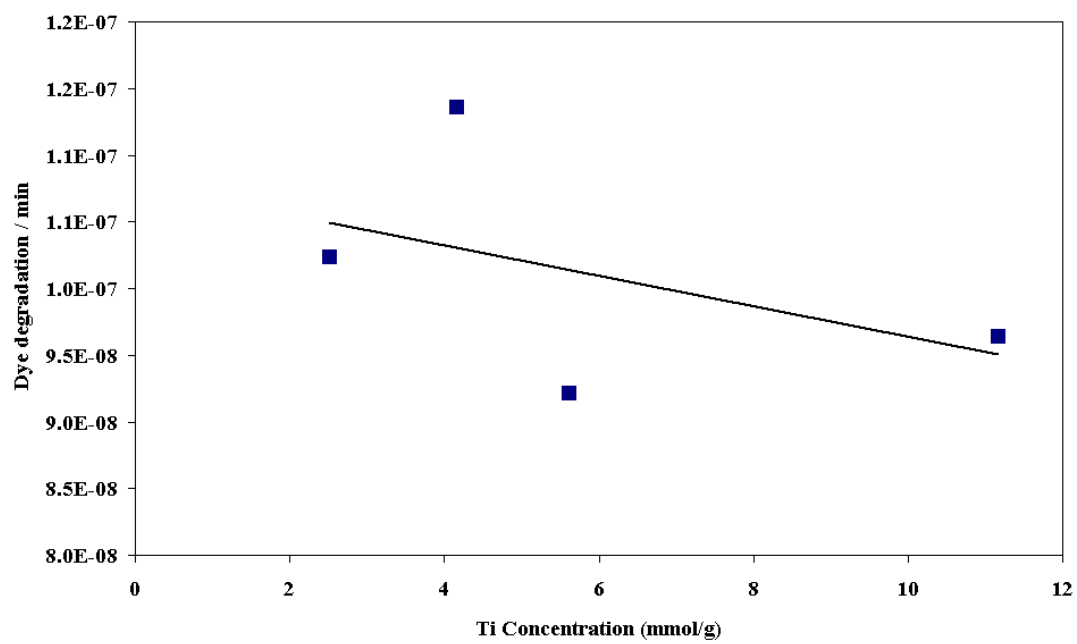


Figure 7